

Analysis of the Image Signal Modulation and Noise Characteristics of Laser Printers

Peter D. Burns

Research Laboratories—Commercial and Information Systems Group, Eastman Kodak Company, Rochester, New York 14650

An analysis is given of the image modulation and noise characteristics of a laser printer via a simple physical model. The model includes the effects of quantization, laser modulation, intensity noise, and image recording. The image signal-to-noise requirements for a printer depend on the applications. For quantum-limited imaging systems these requirements can be expressed as a noise equivalent quantum (NEQ) input exposure. The model is used to describe the NEQ for a system that has a laser printer as its final stage. Example calculations relevant to continuous-tone imaging are given.

Journal of Imaging Science 31: 74–81 (1987)

Introduction

Electronic imaging systems often employ several technologies to detect, process, and display image information. To understand limitations present and opportunities available during design of these integrated systems, a consistent systematic analysis of signal modulation and noise degradation is essential. Signal-to-noise ratio (SNR) techniques are well suited to this task, which is simplified since signal transformations are often sequential.¹ Our aim here is to describe the effect of the signal modulation and noise sources on the image signal. We start by developing an imaging model for a printer that includes quantization, laser modulation, and recording of the output image. A useful review of laser printing and related technologies can be found in Ref. 2.

The SNR requirements for a laser printer are set by the intended system application. Interpretation of these goals requires that the system imaging performance be expressed in equivalent form. One system goal is the detection and display of the largest amount of information available at the input exposure. This is often a criterion when exposure is quantum limited, as it is for many medical imaging applications. In that case, the output SNR is often expressed in terms of noise equivalent quantum exposure (NEQ).^{3–5}

The physical imaging model of the printer can be used to set design parameters to be consistent with overall system requirements. As an example, we consider a quantum limited detector-printer system whose SNR requirements can be expressed in terms of NEQ and detective quantum efficiency (DQE).

A laser printer receives the input image in digital form and converts it to an analog function of time, which is used to modulate the laser exposure intensity. The signal, prior to writing, is a one-dimensional transformation (either electronic or optical) of the intended image. In general, the effect of signal processing on the final image is not isotropic and depends on the specific writing configuration (e.g., pixel size).^{6,7} We can, however, include the equivalent descriptors

(i.e., transfer functions and noise sources) in terms of output image dimensions, given a particular writing scheme. Two types of noise sources are considered; those independent of the signal, and those that are a function of its mean value. This is in contrast with aliasing errors⁶ since they will also be functions of the image spectrum (autocorrelation).

We will also limit our SNR analysis to systems exhibiting symmetrical spread functions, fully characterized by their MTFs. Significant image degradation can be caused by, e.g., an asymmetrical beam profile, but this will not necessarily reduce the NEQ. This is because NEQ describes the SNR for the statistical ensemble of input signals and therefore averages image information over all phase angles at a given spatial frequency. The signal transfer model of the next section, however, is generally applicable. For imaging systems with asymmetrical spread functions each component MTF must be substituted with the corresponding complex optical transfer function. Signal degradation can then be quantified for specific signals of interest.

Model

Figure 1 shows a schematic representation of an imaging system including an output printer. After the sensor the image is sampled and digitized (quantized); we assume that the quantization levels are equally spaced in exposure and that no image compression is involved. The digital signal is converted to analog form, which now includes quantization noise n_b . The analog signal q modulates (multiplies) the laser output. The spread function associated with the modulator includes image blurring that occurs in the fast-scan direction due to sample and hold interpolation between pixel values. We make the assumption that the laser exposure source can be represented by a continuous intensity profile function, and that the exposure is sufficient that the modulation step can be described by the multiplication of the function by the pixel value. If, however, the laser emits a very low exposure, we need to address the statistics of individual photon amplification and scattering events.⁸ Since the modulated laser is scanned across the photosensitive recording material, the finite beam profile (width) introduces an effective spread function into the signal path.

Laser intensity noise can arise from many physical sources,^{9–11} and each laser type exhibits unique noise characteristics. Periodic fluctuations of laser intensity and line position can seriously degrade image quality by introducing one-dimensional stripes or “banding” artifacts into the recorded image.¹² For this reason, compensation for these error sources is often achieved through modulating electronics.^{12–14} In general, however, there will be uncompensated intensity noise and we approximate this by a stochastic source. It is assumed that the beam intensity varies as a function of time about the mean beam profile. We model this as the multiplication of the beam intensity by a random variable. This has the effect of varying the spread function associated with the scanned laser beam as the image is written. Two digital image-restoration techniques for similar

This paper is based on a presentation given at the SPSE Imaging Symposium in Arlington, VA, Nov. 1985. Received May 15, 1986; revised Sept. 22, 1986.

© 1987, SPSE—The Society for Imaging Science and Technology.

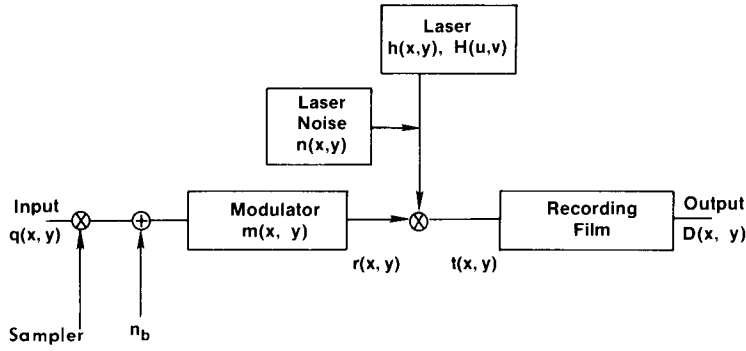


Figure 1. Schematic signal diagram for laser printer.

types of distortion have been described by Ward and Saleh.¹⁵

The modulated laser is used to expose the recording material. In general, the choice of recording material will be influenced by system SNR requirements rather than those for signal modulation transfer.¹⁶

Analysis

The printer modulation transfer function (MTF), from detected input signal to output exposure incident on the recording material, can be expressed in terms of the MTF of each stage,

$$T_p(u, v) = M(u, v) H(u, v), \quad (1)$$

where M is the modulator MTF and H is the normalized Fourier transform modulus of the beam profile. There may be several different causes of reduced signal modulation in laser printers, such as beam truncation by the deflector or A/D converter electronics. For our analysis we consider the modulator MTF, $M(u, v)$, as providing a lumped description of these effects.

We now analyze the noise due to sources identified in the imaging model. It is assumed that the laser printer input is a stationary random variable resulting from the detection of a uniform input exposure. This can be represented as the sum of a constant mean value plus a zero mean stochastic component,

$$\tilde{q}(x, y) = \mu_q + \tilde{n}_q(x, y),$$

where μ_q indicates the mean, or expectation, of $q(x, y)$.

To minimize the introduction of rounding errors, most digital imaging systems use various levels of bit precision for detection, processing, and display. For example, 12 or 16 bits may be used for image processing, but only 8 for modulation of the display. The value of bit precision is chosen as an integral part of any image compression scheme. We consider the quantization effects of a single level of bit precision. The choices of the number of levels and the exposure interval associated with each level are usually made to minimize visible quantization artifacts in large, low-contrast image areas.¹⁷ For continuous-tone printing this may require more than 8 bits, with the size of each interval being a nonlinear function of input exposure. Since we are not addressing aliasing noise due to sampling or interpolation, the process of sampling, digitizing, and reconstructing a continuous signal can be modeled as the addition of a zero mean quantization noise source. Making the usual assumption of a uniform distribution for error, the variance is given by¹⁸

$$\sigma_b^2(i) = \frac{\Delta q(i)}{12 XY} \text{exposure}^2 \text{ mm}^2,$$

where $\Delta q(i)$ is the quantization interval, and X and Y are the pixel sampling intervals in each dimension. For the special case of uniform quantization

$$\sigma_b^2 = \frac{E_{\text{max}}}{12 XY 2^b} \text{exposure}^2 \text{ mm}^2,$$

where E_{max} is the maximum exposure, b is the number of bits used, and X and Y are the pixel sampling intervals in each image dimension. The output of the digital-to-analog converter is

$$r(x, y) = \{\mu_q + \tilde{n}_q(x, y) + \tilde{n}_b(x, y)\} \otimes m(x, y),$$

where \otimes indicates convolution and m is the modulator spread function. This quantization noise will be uncorrelated for all signals except those that occupy very few levels, i.e., highly correlated signals.¹⁹ The corresponding noise power spectrum has a component due to each noise source

$$S_r(u, v) = \{S_q(u, v) + S_b(u, v)\} M(u, v)^2, \quad (2)$$

where S indicates noise power spectrum. To understand the contribution of laser intensity fluctuations to image noise, we first express the modulated exposure in terms of the input signal and beam intensity profile. This can be represented as the convolution of the continuous signal with the beam profile function. This was implicit in Eq. (1). If the beam intensity fluctuates during image writing, it can be described as the multiplication of $h(x, y)$ by a random variable, whose mean value is unity. In general, this noise source will not be independent of the written signal. We will assume that the laser noise is proportional to the average modulated signal. This is given by

$$\tilde{n}(x, y, q) = \mu_q \tilde{n}(x, y).$$

Since the beam intensity fluctuations at a point affect the written pixel exposure at that position, the beam intensity fluctuations can be included in the convolution as

$$t(x', y') = \int_{-\infty}^{\infty} \int_{-\infty}^{\infty} \tilde{r}(x, y) \tilde{n}(x, y) h(x - x', y - y') dx dy, \quad (3)$$

where the mean of $n(x, y)$ is unity. It can be shown (see Appendix II) that

$$\mu_t = \mu_r \quad (4)$$

$$\begin{aligned} \sigma_t^2 = & \iint_{-\infty}^{\infty} \iint_{-\infty}^{\infty} R_r(x_1 - x_2, y_1 - y_2) R_n(x_1 - x_2, y_1 - y_2) h(x_1, y_1) \\ & \cdot h(x_2, y_2) dx_1 dx_2 dy_1 dy_2 + \mu_r^2 \int_{-\infty}^{\infty} \int_{-\infty}^{\infty} S_n(u, v) H^2(u, v) du dv \\ & + \mu_n^2 \int_{-\infty}^{\infty} \int_{-\infty}^{\infty} S_r(u, v) H^2(u, v) du dv, \end{aligned} \quad (5)$$

where R indicates the autocovariance function. The exposure noise power spectrum is given (see Appendix II) by

$$S_t(u,v) = \{[S_r(u,v) \odot S_n(u,v)] + \mu_r^2 S_n(u,v) + \mu_r^2 S_r(u,v)\} H^2(u,v),$$

or from Eq. (2), and noting that μ_n equals unity

$$S_t(u,v) = \{([S_q(u,v) + S_b(u,v)]M^2(u,v) \odot S_n(u,v) + \mu_r^2 S_n(u,v) + [S_q(u,v) + S_b(u,v)]M^2(u,v))\} H^2(u,v). \quad (6)$$

Examination of Eq. (6) reveals that the convolution term of the RHS will be much smaller in magnitude than the others. If we assume the term is negligible and note $\mu_q = \mu_r$, then

$$S_t(u,v) = \{\mu_q^2 S_n(u,v) + [S_q(u,v) + S_b(u,v)]M^2(u,v)\} H^2(u,v). \quad (7)$$

As indicated earlier, the specific writing configuration used can affect signal modulation and noise propagation for laser printers. To make the analysis general and ease interpretation, the model components have been expressed in terms of the dimensions of the written image. However, we measure and specify the subsystem properties in different terms. For example, the laser fluctuations occur as a (stochastic) function of time, not distance. The equivalent noise source is $n(t)$ with power spectral density, $S_n(w)$, a function of w hertz having units of J^2/sec . It is only by considering the scanning sampling interval and velocity in x and y directions that we can express $S_n(u,v)$ in terms of $S_n(w)$. For a raster scanning configuration, we can assume that the time covariance function

$$R_n(\tau) = 0 \quad \text{for } \tau > L,$$

where L is the time for the laser to scan one image line. It can be shown that

$$S_n(u,v) = \frac{S_n(w)}{v_x Y},$$

where v_x is the fast scan velocity. The constant factor is found after consideration of the units of time and distance. More importantly, the noise power spectrum $S_n(u,v)$ is anisotropic except when $S_n(w)$ is constant.

Recorded Image. The final step of the laser writer is exposure and development of the photosensitive material. In order to extend the signal and noise transfer analysis to the output image, we need a corresponding description of the material. A simple model²⁰ applied to photographic film assumes that the written "signal" is first modified by a spread function (MTF) and is then degraded by additive film granularity noise. The printer-film MTF, from detected signal to output image, is

$$\text{MTF}_{pf}(u,v) = M(u,v)H(u,v)T_f(u,v), \quad (8)$$

where T_f is the MTF of the recording film. The power spectrum of the output density fluctuations is given by

$$S_f(u,v) = \left\{ \frac{\gamma \log_{10} e T_f(u,v)}{\mu_t} \right\}^2 S_t(u,v) + WS_f(u,v) \quad (9)$$

in units of $\text{Density}^2 \mu\text{m}^2$, where γ is the slope of the characteristic D -log E curve at exposure μ_t , WS_f is the Wiener spectrum of the film granularity.

This model strictly applies when the "signal" fluctuations, t , are statistically independent of those due to the recording materials. Most printing systems only approximate this behavior since the fluctuations of the recording materials are a function of the (mean) value of the signal to be printed at any point in the image. In general, the lower the recording materials noise levels compared to signal fluctuations, the more realistically the model describes the performance of continuous-tone printing systems.

All the elements of the laser printer imaging model have now been developed. It should be emphasized, however, that the model and associated expressions are generally only valid for small deviations about the specified mean signal value. In addition, several parameters [e.g., $n(x,y)$ and WS_f] vary with the mean signal level. The model can be used to investigate the effect of various design parameters on image signal and noise. First, however, it is useful to describe the imaging performance of such a system in terms of a SNR measure, NEQ.

Noise Equivalent Quanta

The imaging performance of optical detectors is often described in terms of DQE.³ The corresponding SNR characteristics of an image, whether in optical or electronic form, can be expressed in terms of NEQ.^{4,5} We consider the case of a laser writer used in conjunction with an exposure limited detector. Figure 2 shows a system comprised of an image detector, a laser writer, and a recording medium. For many digital imaging systems there could be an additional image processing step between the detector and the writer. The detector is characterized by its DQE which is a function of spatial frequency and mean exposure, Q . First, we address the system up to the modulated laser exposure incident on the recording medium.

The NEQ at the output of the detector can be expressed as³

$$\text{NEQ}_d = \frac{Q^2 T_d^2 G_d^2}{S_q} \quad (10)$$

and

$$\text{DQE}_d = \frac{\text{NEQ}_d}{Q},$$

where G_d is the gain dq/dQ .

The laser printer is described by MTF (T_p), input-output gain (G_p) and noise sources as given in the above model. We can define a printer Wiener spectrum as that exposure noise power spectrum present when the input, μ_q , is noise-free. From Eqs. (1) and (7),

$$WS_p = T_p [S_b + (\mu_q^2 S_n / M^2)]. \quad (11)$$

The exposure noise spectrum for a detector-printer system is, from Eq. (7),

$$S_t = T_p^2 G_p^2 S_q + WS_p.$$

The detector-printer exposure NEQ is therefore

$$\text{NEQ}_{dp} = \frac{[QT_d T_p G_d G_p]^2}{G_p^2 T_p^2 S_q + WS_p}.$$

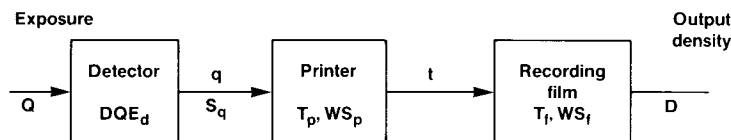


Figure 2. Imaging system with quantum input exposure.

This can be written in terms of the detector NEQ,

$$NEQ_{dp} = \frac{NEQ_d}{1 + (WS_p/S_q G_p^2 T_p^2)} \quad (12)$$

We continue with this approach to incorporate the effect of the imaging characteristics of the recording film on the detected NEQ. We assume, as in Eq. (9), that the output noise power spectrum for the written image is

$$S_d = T_f^2 G_f^2 S_t + WS_f \quad (13)$$

or

$$S_d = [G_f T_f G_p T_f]^2 S_q + [G_f T_f]^2 WS_p + WS_f,$$

where (as above) we used the linear gain G_f . The final NEQ can be written as

$$NEQ_{dpf} = \frac{NEQ_d}{1 + (WS_p)/(S_q [T_p G_p]^2) + (WS_f)/(S_q [T_p G_p T_f G_f]^2)} \quad (14)$$

Equations (12) and (14) express the NEQ for the written image in terms of the detected NEQ and laser printer model parameters. The printer MTF is given in Eq. (1) and the noise sources are given in Eq. (7). These were incorporated via Eq. (11) into the NEQ in Eq. (12). The film MTF and granularity noise were included in the NEQ via Eq. (13).

Computed Examples

The imaging model for the laser printer is used in several sample calculations below. First, we calculate the output Wiener spectrum due to printer noise sources, ignoring the film granularity. We assume that the input signal is constant, i.e., σ_q is zero. In this case, the signal would only occupy one quantization level and, therefore, S_b would be zero. We include a quantization noise, however, since we are interested in understanding the printer noise characteristics in the context of image writing. The printer parameters are as follows: Gaussian laser beam, $\sigma_L = 0.045$ mm, sampling distances $X = Y = 0.1$ mm, and a sample and hold modulator.

The sensitometric characteristics of the hardcopy recording film are shown in Fig. 3. We further assume that the film MTF is constant over the spatial frequencies of interest. The system MTF, given by Eq. (1) and shown in Figs. 4 and 5, is anisotropic due to the modulator MTF, $M(u) = \text{sinc}(uX)$.

If we ignore the contribution due to film granularity, the output Wiener spectrum is calculated as in Eq. (9) with $WS_f(u)$ equal to zero. In Fig. 6, this is shown versus spatial frequency at a density of 1, for uncorrelated (white) laser noise equal to one percent and various numbers of A/D bits. The quantization levels have been set in equal log exposure increments over two decades. The corresponding zero frequency values are plotted versus mean density in Fig. 7. To

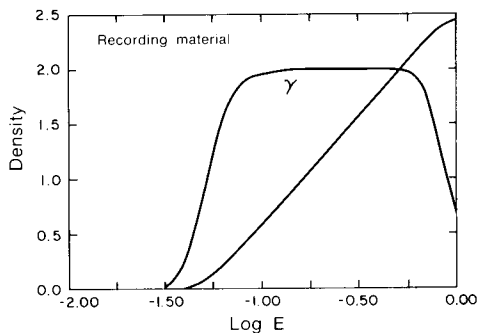


Figure 3. Recording film sensitometry for the example.

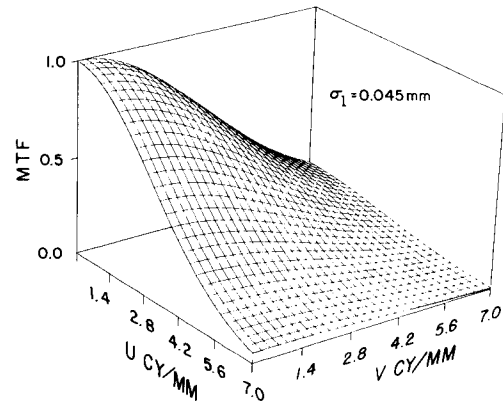


Figure 4. Example printer MTF.

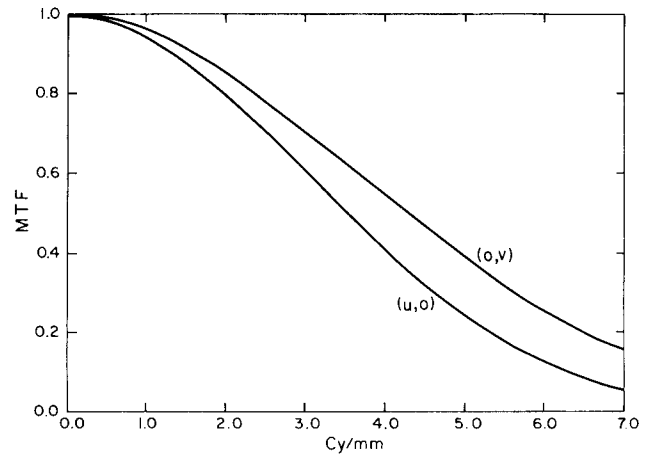


Figure 5. Example printer MTF cross-section.

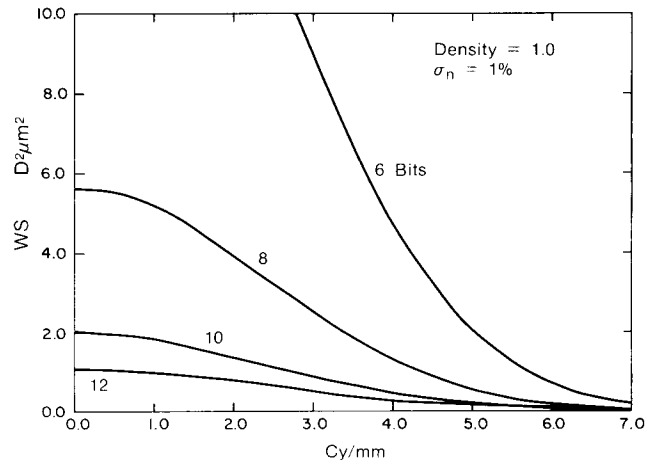


Figure 6. Wiener spectrum versus spatial frequency, ignoring film granularity, for a mean density = 1.0 and $\sigma_n = 1\%$.

show the effect of the laser intensity fluctuations, the Wiener spectrum was then calculated for various values of σ_n and 8 bits (Fig. 8).

The entire Wiener spectrum versus spatial frequency and exposure surface is shown in Fig. 9. The spatial frequency axis is along the diagonal where $u = v$ to allow it to be represented in one dimension, where the modulator and spot profile characteristics determine the surface envelope. Film sensitometry determines the shape of the surface in the exposure direction.

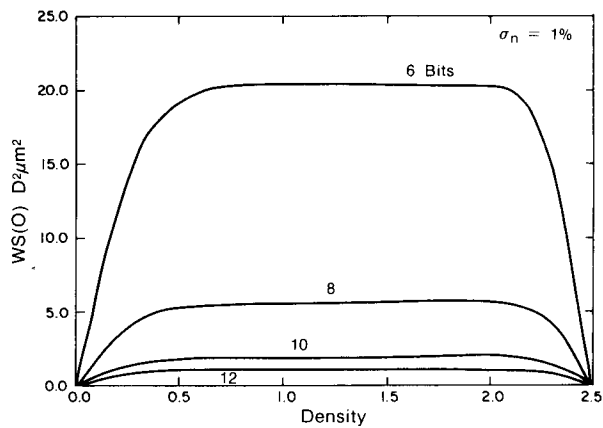


Figure 7. Wiener spectrum at zero frequency, ignoring film granularity for $\sigma_n = 1\%$.

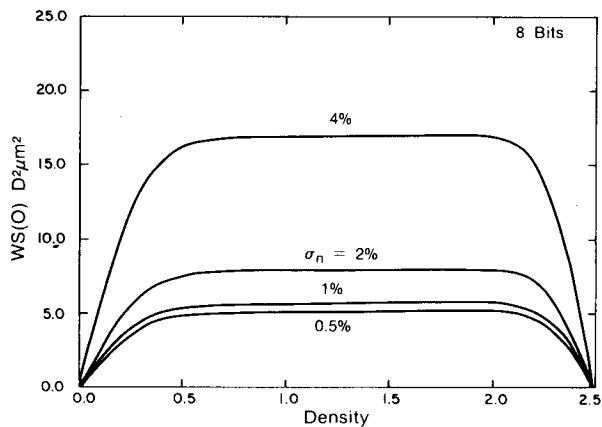


Figure 8. Wiener spectrum at zero frequency, ignoring film granularity for 8 bits.

We can include the noise component due to the recording material if we have a model for film granularity. A simple model, due to Siedentopf, describes noise resulting from random image particles.²¹ The low frequency value of the Wiener spectrum of the recording material is given by

$$WS_f(0) = \log_{10} e D a'$$

where D is the average density and a' is the effective projected area of the assumed monosized image particles of the recording material. We assume a' is about twice the physical

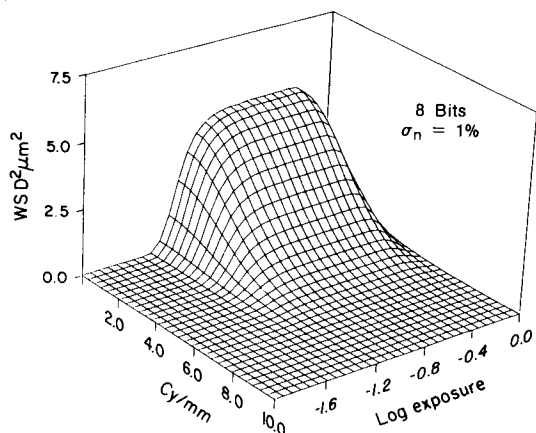


Figure 9. Wiener spectrum surface for example printer design ignoring film granularity.

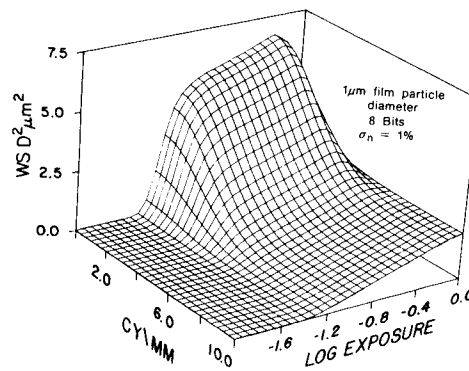


Figure 10. Wiener spectrum surface with the addition of the recording film granularity component.

particle size due to optical scattering. Figure 10 shows the resulting calculated Wiener spectrum surface for this example, adding the component due to the granularity of the recording materials for a $1\text{-}\mu\text{m}$ particle diameter. This component is assumed to be constant over all spatial frequencies of interest, as is the MTF of the recording material.

We can extend this example by calculating the NEQ that would result from the laser printing of images from the detection of a quantum input exposure. First, as in the Noise Equivalent Quanta Section, we need to specify the exposure, Q , and DQE of the detector. Alternatively, we can specify the NEQ of the detected exposure, NEQ_d . For this example, the detector is assumed to accurately count a fixed fraction of the incident quanta so the detected NEQ is merely

$$NEQ_d = \eta Q,$$

where η is a constant. This is shown in Fig. 11 as a surface rising with exposure. The maximum detected exposure is 5×10^5 quanta/mm² corresponding in the figures to an input exposure of 10^6 quanta/mm², implying a detector DQE value of 0.5.

We do not want the image NEQ to be significantly degraded by the printer. Consider a printer similar to the previous example with sampling intervals (0.1 mm), spot shape, laser noise (1%), and recording material sensitometry (with maximum exposure of 10^6 quanta/mm²). Figure 12 shows the calculated output Wiener spectrum for a printer using 10 bits to modulate the laser exposure of recording material with $0.5\text{-}\mu\text{m}$ diameter developed particles. The shape is similar to the previous example in Fig. 10.

The NEQ was calculated for the exposure image, $t(x,y)$, shown in Fig. 13. The laser printer reduces the image NEQ primarily at high values of exposure and spatial frequency as shown in Figs. 11 and 13. To assess SNR degradation due to

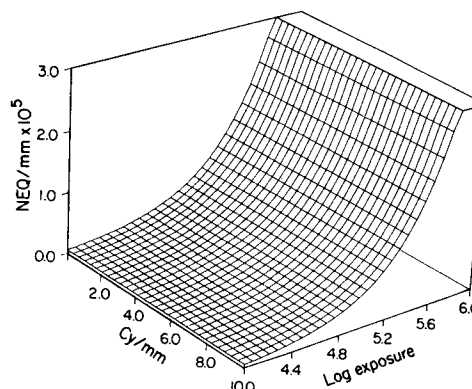


Figure 11. NEQ surface for detected input quantum exposure.

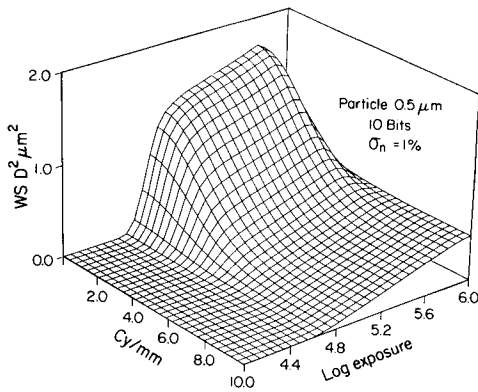


Figure 12. Wiener spectrum surface for the second example printer design.

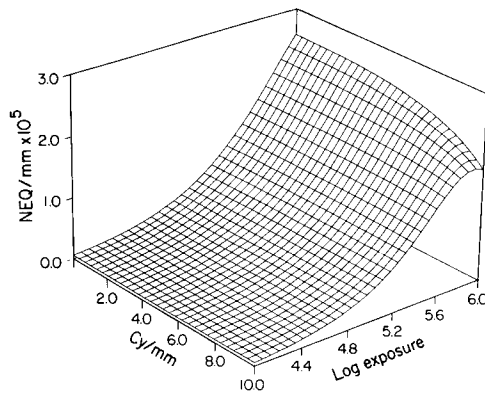


Figure 13. NEQ surface for the written exposure image.

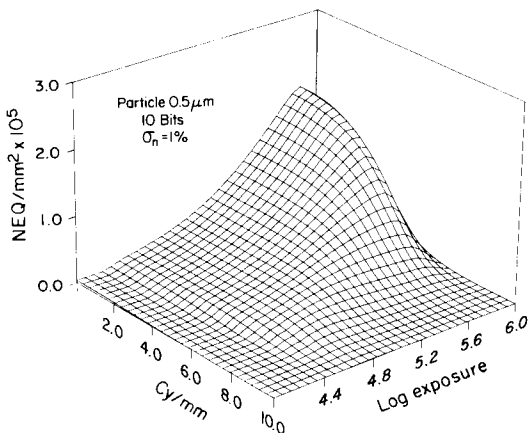


Figure 14. NEQ surface for the printed image.

the addition of film granularity, NEQ was calculated for the output written image assuming a particle diameter of $0.5 \mu\text{m}$. The resulting surface shown in Fig. 14 is quite different in shape from the previous one. The reduction in NEQ with spatial frequency is due to the constant Wiener spectrum of the recording materials. Since the signal modulation decreases with spatial frequency, SNR measured by NEQ decreases approximately as MTF squared.

Conclusions

An analysis has been given of the image signal modulation and noise characteristics for a laser printer via a simple physical model. The model provides a way to interpret several key design choices in terms of their effect on image quality.

The approach taken is consistent with established techniques for the design and evaluation of imaging systems, such as MTF and Wiener spectrum. For quantum limited applications, SNR requirements are often expressed as NEQ input exposure. If a laser printer is the final step in such a system, then its imaging characteristics can be included as part of the description. In this way, the hardcopy display can be designed in the context of the system image quality requirements. \blacktriangle

Acknowledgement. I thank D. Haas for his suggestions and M. Rabbani for help in refining the initial approach.

References

1. C. L. Fales, F. O. Huck, and R. W. Samms, *Appl. Opt.* **6**: 872(1984).
2. J. C. Urbach, T. S. Fisli, and G. K. Starkweather, *Proc. IEEE* **70**: 597(1982).
3. (a) R. C. Jones, *Photogr. Sci. Eng.* **2**: 57(1958); (b) R. Shaw, *J. Photogr. Sci.* **11**: 199(1963); (c) J. C. Dainty and R. Shaw, *Image Science*, Academic Press, London, 1974, chap. 5.
4. For example, (a) P. C. Bunch, R. Shaw, and R. L. VanMetter, *Proc. SPIE* **454**: 154(1984); (b) R. Shaw and R. L. VanMetter, *Proc. SPIE* **535**: 184(1985).
5. For example, R. Shaw and R. L. VanMetter, *Proc. SPIE* **535**: 128(1984).
6. F. O. Huck, N. Halyo, and S. K. Park, *Appl. Opt.* **19**: 2174(1980).
7. J. R. Sullivan, *Proc. 2nd Intl. Congress on Advances in Non-Impact Printing Technol.* SPSE, 1984, p. 48.
8. P. L. Dillon, J. F. Hamilton, M. Rabbani, R. Shaw, and R. L. VanMetter, *Proc. SPIE* **535**: 130(1984).
9. D. E. McCumber, *Phys. Rev.* **141**: 306(1966).
10. T. L. Paoli and J. E. Ripper, *Phys. Rev. A* **2**: 2551(1970).
11. A. D. Berg and J. P. Wheeler, *Opt. Eng.* **15**: 84(1976).
12. F. Bestenreiner, U. Geis, J. Helmberger, and K. Stadler, *J. Appl. Photogr. Eng.* **2**: 86(1976).
13. F. S. Chen, M. A. Karr, and P. W. Shumate, *Appl. Opt.* **17**: 2219(1978).
14. R. L. Trantow, *Proc. SPIE* **299**: 18(1981).
15. R. K. Ward and B. E. A. Saleh, *J. Opt. Soc. Am. A* **2**: 1254(1985).
16. R. Shaw and P. D. Burns, *Proc. 2nd Intl. Congress on Advances in Non-Impact Printing Technol.* SPSE, 1984, p. 127.
17. F. Bestenreiner, J. Freund, U. Geis, and J. Helmberger, *Proc. 1st Intl. Congress on Advances in Non-Impact Printing Technol.* SPSE, 1981, p. 1251.
18. A. V. Oppenheim and R. W. Schaffer, *Digital Signal Processing*, Prentice-Hall, Englewood Cliffs, NJ, 1975, pp. 409-413.
19. W. R. Bennett, *Bell Syst. Tech. J.* **27**: 446(1948).
20. E. C. Doerner, *J. Opt. Soc. Am.* **52**: 669(1962); see also J. C. Dainty and R. Shaw, *Image Science*, Academic Press, London, 1974, chap. 8.
21. H. Siedentopf, *Phys. Z.* **38**: 454(1937).

Appendix I

Table of Symbols

b	= number of bits used for A/D and D/A conversion.
σ_b^2	= quantization noise variance.
$S_b(u,v)$	= quantization noise power spectrum.
$G_d(Q)$	= input-output gain of detector.
$T_d(u,v)$	= detector MTF.
NEQ_d	= NEQ at output of detector.
DQE_d	= detective quantum efficiency of detector.
NEQ_{dp}	= NEQ at output of detector-printer system.
NEQ_{dpp}	= NEQ at hardcopy output of detector-printer.
$T_f(u,v)$	= MTF of recording material.
γ	= slope of density-log exposure characteristic of recording material.
G_f	= slope of density-exposure characteristic of recording material.
$WS_f(u,v)$	= Wiener spectrum of recording materials granularity.
$H(u,v)$	= normalized Fourier transform of beam profile.
L	= total length of scan line across the image.
$m(x,y)$	= modulator spread function.
$M(u,v)$	= modulator MTF.
$n(x,y)$	= laser exposure noise (random variable).
$R_n(x,y)$	= laser exposure noise autocovariance function.
$S_n(u,v)$	= laser exposure noise power spectrum.
G_p	= input-output gain of printer.

$T_p(u,v)$	= printer MTF from detected input signal to exposure to recording material.
$WS_p(u,v)$	= printer Wiener spectrum (see text).
$MTF_{pr}(u,v)$	= combined MTF of printer and recording material.
Q	= mean exposure to detector.
$q(x,y)$	= printer input signal.
$S_q(u,v)$	= printer input power spectrum.
$r(x,y)$	= output of D/A converter.
$S_r(x,y)$	= D/A converter output power spectrum.
$t(x,y)$	= modulated exposure to recording film.
$S_t(u,v)$	= modulated exposure power spectrum.
v_x	= scanning velocity in fast scan direction.
X,Y	= pixel sampling distance in fast and slow (page) scan direction.
σ_L	= Gaussian beam shape parameter.

Appendix II

Modulation of Time Varying Spread Function. A one-dimensional analysis is presented; however, the results are easily extended to two-dimensional images. An output signal $t(x)$ results from the modulation of $h(x)$ by the input signal, $r(x)$ as follows

$$t(x) = \int r(x')h(x' - x)dx' \quad (\text{A-1})$$

The laser beam profile (spread function) is $h(x)$. If the laser intensity fluctuates during image writing, this can be modeled as the presence of a random (variable) component that multiplies the input signal just prior to modulation (convolution). The random variable, $n(x)$, has a mean value of unity and enters Eq. (A-1) as

$$t(x) = \int r(x')n(x')h(x' - x)dx', \quad (\text{A-2})$$

where $t(x)$ is now also a random variable. We start by assuming that the input signal, $r(x)$, and noise source, $n(x)$, are independent stationary random processes. To simplify treatment of the units of exposure, we also assume that

$$\int_{-\infty}^{\infty} h(x)dx = 1.$$

This last assumption allows us to ignore units of intensity and exposure.

Mean

From Eq. (A-2) the expectation

$$E[t(x)] = \int E[r(x')n(x')]h(x' - x)dx.$$

Since $r(x)$ and $n(x)$ are independent,

$$E[t(x)] = \mu_r \mu_n. \quad (\text{A-3})$$

Variance

$$\text{Var}[t(x)] = E[t^2(x)] - E[t(x)]^2 \quad (\text{A-4})$$

the first term of the RHS is

$$E[t^2(x)] = \iint E[r(x'_1)r(x'_2)]E[n(x'_1)n(x'_2)] \\ \times h(x'_1 - x)h(x'_2 - x)dx'_1dx'_2.$$

This is simplified since

$$E[r(x'_1)r(x'_2)] = R_r(x'_1 - x'_2) + \mu_r^2, \quad (\text{A-5})$$

where $R_r(x)$ is the autocovariance function (*acv*) of $r(x)$. From Eqs. (A-3) and (A-5), Eq. (A-4) becomes

$$\text{Var}[t(x)] = \iint R_r(x'_1 - x'_2)R_n(x'_1 - x'_2)h(x'_1 - x) \\ \times h(x'_2 - x)dx'_1dx'_2 \\ + \mu_r^2 \iint R_n(x'_1 - x'_2)h(x'_1 - x)h(x'_2 - x)dx'_1dx'_2 \\ \times \mu_n^2 \iint R_r(x'_1 - x'_2)h(x'_1 - x)h(x'_2 - x)dx'_1dx'_2. \quad (\text{A-6})$$

This equation for the variance of $t(x)$ can be rewritten in a shift-invariant form by a change of variables. Let

$$y_1 = x'_1 - x$$

$$y_2 = x'_2 - x.$$

The first term is

$$\iint R_r(y_1 - y_2)R_n(y_1 - y_2)h(y_1)h(y_2)dy_1dy_2. \quad (\text{A-7})$$

The second term can be rewritten using the same change of variables. Expressing the *acv* function in terms of its Fourier transform gives

$$\mu_r^2 \iiint S_n(u)e^{ju(y_1 - y_2)}h(y_1)h(y_2)dy_1dy_2du, \quad (\text{A-8})$$

where $S_n(u)$ is the power spectral density of $n(x)$, and $j = \sqrt{-1}$. Expression (A-8) can be rewritten by integrating over y_1 and y_2 to yield

$$\mu_r^2 \int S_n(u)|H(u)|^2du. \quad (\text{A-9})$$

The third term of Eq. (A-6) is similar to the second term and can be expressed as

$$\mu_n^2 \int S_r(u)|H(u)|^2du. \quad (\text{A-10})$$

The substitution of Eqs. (A-7), (A-9), and (A-10) into Eq. (A-6) gives the desired result of Eq. (5).

Noise Power Spectrum

To find the power spectrum of $t(x)$ we first need the *acv*,

$$R_t(\tau) = E[t(x)t(x - \tau)] - E[t(x)]^2. \quad (\text{A-11})$$

The first term is

$$E[t(x_1)t(x_2)] = \iint [R_r(x'_1 - x'_2) + \mu_r^2][R_n(x'_1 - x'_2) + \mu_n^2] \\ \cdot h(x'_1 - x_1)h(x'_2 - x_2)dx'_1dx'_2, \quad (\text{A-12})$$

where $\tau = x_1 - x_2$.

The RHS of Eq. (A-12) can be expanded into four integral terms. The first is

$$\iint R_r(x'_1 - x'_2)R_n(x'_1 - x'_2)h(x'_1 - x_1)h(x'_2 - x_1)dx'_1dx'_2.$$

This can be rewritten by the change of variables

$$x_1 = x_2 - \tau$$

$$z_1 = x'_1 - x_2$$

$$z_2 = x'_2 - x_2$$

to give

$$\iint R_r(z_1 - z_2)R_n(z_1 - z_2)h(z_1 - \tau)h(z_2)dz_1dz_2.$$

Taking the Fourier transform of this expression and integrating with respect to τ gives

$$H(u) \iint R_r(z_1 - z_2)R_n(z_1 - z_2)e^{juz_1}h(z_1)dz_1dz_2. \quad (\text{A-13})$$

This is simplified by defining

$$R_{rn}(z_1 - z_2) \equiv R_r(z_1 - z_2)R_n(z_1 - z_2).$$

The expression (A-13) can now be expressed as

$$H(u)H^*(u)S_{rn}(u),$$

where $*$ indicates complex conjugate and S_{rn} is the Fourier transform of R_{rn} . This is now equal to

$$[S_r(u) \otimes S_n(u)]|H(u)|^2 \quad (\text{A-14})$$

since $r(x)$ and $n(x)$ are independent.

The second term of Eq. (A-12) is

$$\mu_r^2 \iint R_n(x'_1 - x'_2)h(x'_1 - x_1)h(x'_2 - x_2)dx'_1dx'_2.$$

This can be written in terms of the Fourier transform of $R_n(x)$ to give

$$\mu_r^2 \iiint S_n(u)h(x'_1 - x_1)e^{ju(x'_1 - x_1)}h(x'_2 - x_2)e^{-j(x'_2 - x_2)} \cdot e^{ju(x_1 - x_2)}dx'_1dx'_2du.$$

Integrating with respect to x'_1, x'_2 and letting $x_1 - x_2 = \tau$ gives

$$\mu_r^2 \int S_n(u)|H(u)|^2e^{ju\tau}du.$$

By using Fourier transform properties this can be expressed as

$$\mu_r^2 S_n(u)|H(u)|^2. \quad (\text{A-15})$$

The third term of the RHS of Eq. (A-12) is treated similarly to the second term to give

$$\mu_n^2 S_r(u)|H(u)|^2. \quad (\text{A-16})$$

The fourth term of the RHS of Eq. (A-12) is separable and equal to

$$\mu_n^2 \mu_r^2. \quad (\text{A-17})$$

The substitution of expressions (A-14)–(A-17) into Eq. (A-12) gives the desired result of Eq. (6) of the text.